SERRE GREEN-NAGHDI MODELLING OF WAVE TRANSFORMATION BREAKING AND RUN-UP USING A HIGH-ORDER FINITE-VOLUME FINITE-DIFFERENCE SCHEME

Marion Tissier[1], Philippe Bonneton[1], Fabien Marche[2], Florent Chazel[3] and David Lannes[4]

In this paper, a fully nonlinear Boussinesq model is presented and applied to the description of breaking waves and shoreline motions. It is based on Serre Green-Naghdi equations, solved using a time-splitting approach separating hyperbolic and dispersive parts of the equations. The hyperbolic part of the equations is solved using Finite-Volume schemes, whereas dispersive terms are solved using a Finite-Difference method. The idea is to switch locally in space and time to NSWE by skipping the dispersive step when the wave is ready to break, so as the energy dissipation due to wave breaking is predicted by the shock theory. This approach allows wave breaking to be handled naturally, without any ad-hoc parameterization for the energy dissipation. Extensive validations of the method are presented using laboratory data.

Keywords: Fully nonlinear Boussinesq equations; Wave breaking; Run-up; Hybrid method; Shock capturing schemes;

INTRODUCTION

Wave transformation in shallow water, and associated processes such as wave-breaking and run-up, play a key role in the nearshore dynamics. Breaking waves and swash motions are the main source of sediment transport in the nearshore. A good estimation of instantaneous wave characteristics, as its steepening and asymmetry is needed to improve the prediction of short-term beach evolution. It is of great interest during storm events, where a given wave can have a significant impact on the coastline. A wave-by-wave approach is also necessary for the study of coastal flooding due to storm waves or tsunamis. Modelling these processes requires a phase-resolving model, able to accurately describe wave-breaking and run-up over strongly varying topographies. The most accurate models for the description of wave breaking are based on the Navier-Stokes equations. However, they are highly computationally demanding, and therefore are not suitable for large scale propagation applications. For this reason, phase-resolving models based on shallow-water equations are still attractive to handle these processes. They are based on Nonlinear Shallow Water (NSWE) or Boussinesq-type (BT) equations.

NSWE models can give a good description of broken-waves, represented as shocks. The use of shock-capturing techniques allows for an accurate representation of broken wave dissipation and swash oscillations without any ad hoc parameterization (Kobayashi et al. 1989, Bonneton 2007, Marche et al. 2007, Brocchini and Dodd 2008). However, since dispersive effects are not taken into account, these equations are restricted to the inner surf and swash zones, where nonlinearities predominate. On the other hand, BT equations account for both nonlinear and dispersive effects at different degrees of accuracy. In the final stages of shoaling and in the surf and swash zones, the wave dynamics is strongly nonlinear. Fully Nonlinear BT equations are required. However, they do not intrinsically include energy dissipation due to wave breaking. They can accurately predict non-breaking wave transformation, including shoaling but they become invalid in the surf zone. Several attempts have been made to introduce wave breaking in Boussinesq models by the mean of ad hoc techniques, which require the prior estimation of empirical parameters (e.g. Madsen et al. 1997, Kennedy et al. 2000, Cienfuegos et al. 2009). FUNWAVE is a well-known example of this kind of models. It gives a good description of wave transformation, but each use of the model implies the prior tuning of several parameters, as the ones determining wave breaking and run-up (see Bruno et al. 2009).

The modelling strategy developed in this paper is based on a coupling of the approaches: breaking waves will be described as shocks by the NSW equations, whereas non-breaking waves will be described by Boussinesq equations. The model is based on the Serre Green-Naghdi (S-GN) equations, which are the

[1] Université de Bordeaux 1, CNRS, UMR 5805-EPOC, Talence F-33405, France
[2] Université de Montpellier 2, UMR CNRS 5149, Place Eugène Bataillon, 34095 Montpellier, France
[3] INSA – Département GMM, 135 avenue de Rangueil, F-31077 Toulouse Cedex 4, France
[4] DMA/CNRS, Ecole Normale Supérieure, 45 rue d'Ulm, 75005 Paris, France

basic Fully Nonlinear Boussinesq equations (Lannes and Bonneton 2009). They can be written as a hyperbolic part, corresponding to the NSW equations, plus a dispersive term. We present here an hybrid finite-volume finite-difference method (Chazel et al. 2010 and Bonneton et al 2010a) which permits to naturally handle wave breaking. The idea is to switch from one set of equations to the other, locally, by skipping the dispersive term when the wave is ready to break. Thus, wave breaking is handled by the NSW equations, and wave energy dissipation due to wave breaking described by the shock theory, without any parameterization.

GOVERNING EQUATIONS

The model is based on the S-GN equations, which are now recognized to be the relevant system to model highly nonlinear weakly dispersive waves propagating in shallow water (see Lannes and Bonneton 2009). These equations can be formulated in term of the conservative variables (h,h**v**) in the following nondimensionalized form (see Bonneton et al. 2010a):

$$\begin{cases} \partial_t h + \varepsilon \nabla \cdot (h\mathbf{v}) = 0 \\ \partial_t (h\mathbf{v}) + gh\nabla\zeta + \varepsilon \nabla \cdot (h\mathbf{v}\otimes\mathbf{v}) = -D, \end{cases} \tag{1}$$

where $\zeta(\mathbf{x},t)$ is the surface elevation, $h(\mathbf{x},t) = 1 + \varepsilon\zeta - b$ the water depth, $b(\mathbf{x})$ the variation of the bottom topography, $\mathbf{v}(\mathbf{x},t) = (u,v)$ the depth averaged velocity. ε=H/ h_0 is the non-linear parameter with H the wave height and h_0 the typical water depth, and μ=$(h_0/\lambda)^2$ the dispersive parameter, with λ the typical wave length. D characterizes non-hydrostatic and dispersive effects and writes:

$$D = -\frac{1}{\alpha} h\nabla\zeta + \left(I + \mu\alpha h T[h,b]\frac{1}{h} \right)^{-1} \left[\frac{1}{\alpha} h\nabla\zeta + \varepsilon\mu h Q_1[h,b](\mathbf{v}) \right], \tag{2}$$

where the linear operator $T[h,b]$ is defined as:

$$T[h,b]W = -\frac{1}{3h}\nabla(h^3\nabla\cdot W) + \frac{1}{2h}\left[\nabla(h^2\nabla b\cdot W) - h^2\nabla b\nabla\cdot W\right] + \nabla b\nabla b\cdot W,$$

and $Q_1[h,b]$ is given by:

$$Q_1[h,b](\mathbf{v}) = \frac{1}{2h}\left[\nabla(h^2(\mathbf{v}\cdot\nabla)^2 b) - h^2((\mathbf{v}\cdot\nabla)(\nabla\cdot\mathbf{v}) - (\nabla\cdot\mathbf{v})^2)\nabla b\right] + ((\mathbf{v}\cdot\nabla)^2 b)\nabla b - T[h,b]((\mathbf{v}\cdot\nabla)\mathbf{v}).$$

The range of validity of the set of equations has been extended to deeper water using the dispersion correction technique discussed in Cienfuegos et al 2006, Chazel et al 2010. α is the resulting optimization parameter and should be taken equal to 1.159 in order to minimize the phase and group velocity errors in comparison with the linear Stokes theory.

The proposed reformulation has two important advantages. First of all, the dispersive term does not require the computation of any third order derivative, allowing for more robust numerical computations. Moreover, the left-hand side of the equations corresponds to the NSWE in their conservative form. The formulation is well-suited for a splitting approach separating the hyperbolic and the dispersive part of the equations.

NUMERICAL SCHEMES

We decompose the solution operator S(•) associated to the equations (1) at each time step dt by the following second order splitting scheme:

$$S(dt) = S1(dt/2)\ S2(dt)\ S1(dt/2), \tag{3}$$

where S1 and S2 are respectively associated to the hyperbolic and dispersive parts of the S-GN equations. S1 is treated using a finite-volume method, and a finite-difference method is used for the dispersive part S2. We briefly present here their main characteristics. The reader is referred to Bonneton et al. 2010a for further details concerning this hybrid method.

Hyperbolic part

Our S-GN model has been developed as an extension of the NSW code SURF_WB (Marche et al 2007), which has been extensively validated for the description of wave propagation in the surf and swash zones. The schemes used in S1 are those which have been developed for SURF_WB: a detailed review of the numerical methods can be found in Marche et al. 2007 and Berthon and Marche 2008. S1 is the solution operator associated with the following system:

$$\begin{cases} \partial_t h + \varepsilon \nabla \cdot (h\mathbf{v}) = 0 \\ \partial_t (h\mathbf{v}) + gh\nabla\zeta + \varepsilon \nabla \cdot (h\mathbf{v} \otimes \mathbf{v}) = 0. \end{cases} \quad (4)$$

This system can be regarded as an hyperbolic system of conservation laws with a source term controlled by the topography variations. It is convenient to rewrite the system (4) in term of the conservative variables $\mathbf{w}={}^t(h,hu)$ in the form (here for the 1D-problem):

$$\partial_t \mathbf{w} + f(\mathbf{w})_x = S(\mathbf{w}),$$

where $f(\mathbf{w})={}^t(hu, hu^2 + 0.5gh^2)$ and $S={}^t(0,-ghb_x)$ the source term. To perform numerical approximations of the weak solutions of this system, we use a high order finite-volume method in conservative variables. More precisely, we use the 4th–order MUSCL reconstruction suggested in Berthon and Marche 2008. Since we aim at computing the complex interactions between propagating waves and topography, including the preservation of motionless steady states, we also embed this approach into a well-balanced scheme (see Audusse et al. 2004). Additional reconstructions are also introduced in order to obtain a positive preserving scheme. The reconstructed quantities are then injected in a positive preserving VFRoe Riemann solver, able to deal with dry areas. The result is a high-order positive preserving well-balanced shock-capturing scheme, able to handle breaking bores propagation as well as moving shorelines without any tracking method.

Dispersive terms

S2 is the solution operator associated with the system:

$$\begin{cases} \partial_t h = 0 \\ \partial_t (h\mathbf{v}) = -D, \end{cases} \quad (5)$$

The system (5) is solved at each time step using a classic finite-difference approach, of fourth-order in space.

Concerning the time discretization, explicit methods are used both in S1 and S2. The systems are integrated in time using a classical fourth-order Runge-Kutta method. When the water depth vanishes, a small routine is applied in order to ensure the stability of the numerical results. When the water depth h is smaller than a threshold h_ε, we impose $h= h_\varepsilon$ and $\mathbf{v}=0$. Extensive validations of the numerical methods for the 1D problem can be found in Bonneton et al. 2010a,b and Chazel et al. 2010. In particular, the propagation of a strongly nonlinear cnoidal wave solution of the S-GN equations has been investigated, demonstrating that the numerical solution converge to the exact one for very small dx. The 2HD extension is left for future work.

WAVE BREAKING

In order to handle wave breaking, we switch from S-GN to NSW equations locally in space and time, by skipping the dispersive step S2 when the wave is ready to break. In this way, we only solve the hyperbolic part of the equation for the wave fronts, and the breaking wave dissipation is determined by the shock theory. The coupling between the two sets of equations is thus performed in a natural way, without implementing any boundary conditions. As we aim at applying our code to realistic incoming waves,

implying different locations of the breaking point, we need to handle each wave individually. We present in this section a simple way to detect wave fronts at each time step, as well as the criterion to initiate and terminate breaking.

Detection of the wave fronts

In order to decide where to suppress the dispersive step, we use the first step S1 of the time-splitting as a predictor to assess the local energy dissipation. It can be expressed as:

$$D_i(x,t) = -\left(\frac{\partial E}{\partial t} + \frac{\partial F}{\partial x}\right), \qquad (6)$$

with $E = \rho / 2\left(hu^2 + g((h+b)^2 - b^2)\right)$ and $F = \rho hu\left(u^2/2 + g(h+b)\right)$ the energy and the energy flux densities. The local dissipation is close to zero in regular wave regions and forms peaks when shocks are appearing. We can then locate the future breaking wave fronts at each time step, and eventually skip the following step S2 in their vicinities. Figure 1 illustrates the evolution of Di for an academic case, concerning a sine wave breaking on a flat bottom (see also Bonneton et al. 2007). Dispersive terms are turned off for this simulation: the wave quickly steepens and breaks, without previous shoaling. Periodic boundary conditions are imposed, and the length of the computational domain is equal to the wave length of the sine wave. The wave height and the corresponding dissipation are plotted at different times, showing that the wave fronts can be easily located as soon as shocks are developing through the location of dissipation peaks.

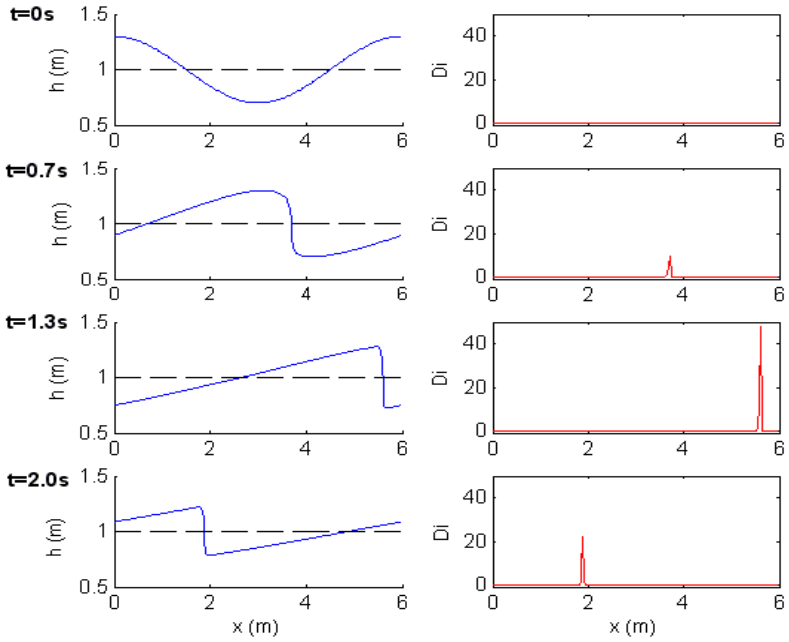

Figure 1. Sine wave propagating over a flat bottom, at different time. ε=0.6; h0=1; Left panel: free surface elevation. Right panel: energy dissipation (Di).

Characterization of breaking

In order to characterize each wave front individually, the local dissipation is integrated over the front and normalized by the theoretical dissipation, given by the shock theory:

D_{th} is the energy dissipated across the shock, with h_1 and h_2 the water heights in front and behind the shock (see Figure 2). From a practical point of view, h_1 and h_2 are approximated by the local minimum and maximum of h which are the closest to the peak of dissipation, and therefore D_{th} is estimated by:

$$D_{th} \approx \frac{\rho g}{4}\left(\frac{g(h_{\min}+h_{\max})}{2h_{\min}h_{\max}}\right)^{1/2} H^3.$$

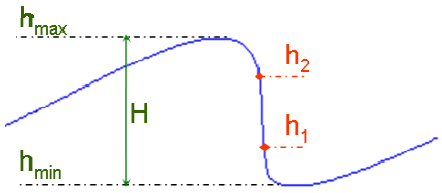

Figure 2. Definition sketch.

The time-evolution of the normalized dissipation $\int_{front} D_i(x,t)dx/D_{th}$ for the previous sine wave is plotted in Figure 3. It is close to zero before breaking, and increases significantly when shocks start developing (h_2–h_1<H). Once the breaker is saturated (i.e. h_2–h_1=H), the normalized dissipation stays close to 1.

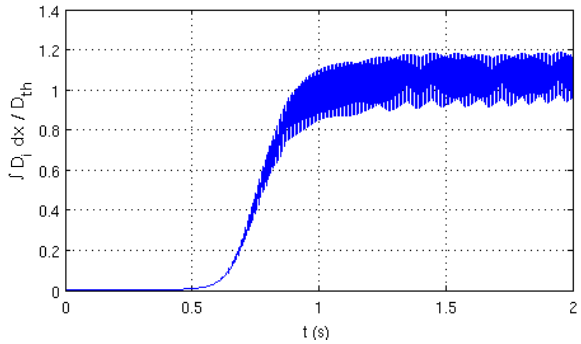

Figure 3. Sine wave propagating over a flat bottom. Time-evolution of the normalized dissipation.

Let's now consider a more realistic test case, corresponding to experiments performed by Ting and Kirby in 1994. Cnoidal waves are propagating and breaking over a beach of slope 1:35. Two simulations are run. For the first test case, the code is run with the full S-GN equations, without any special treatment for wave breaking. The waves keep propagating shoreward to the experimental breaking point without dissipating enough energy, leading to unrealistic wave heights close to the shoreline. As we can see in the left panel of Figure 4, there is an increase of the normalized dissipation in the vicinity of the experimentally observed breaking point, but the transition is not sharp enough to use dissipation as the only criterion to initiate wave breaking. This is mainly due to the presence of the dispersive step S2, which tends to counterbalance the shock formation which occurs during the hyperbolic steps, preventing the shocks to fully develop. This analysis is confirmed by the second test, where a switch to NSWE is performed shoreward to the experimental breaking point. As soon as we suppress the step S2, we observe a fast increase of this dissipation, within a few cells, until the waves are fully broken. These broken waves keep propagating shoreward with a normalized dissipation oscillating around one. Based on this observation, we define a simple criterion to characterize wave fronts. If $\int_{front} D_i(x,t)dx/D_{th} > 0.5$ the wave is already

broken, and if $\int_{front} D_i(x,t)dx/D_{th} \leq 0.5$, the wave is not breaking yet. Thus, we can easily determine at which stage of their transformation the waves are at each time step, without following them.

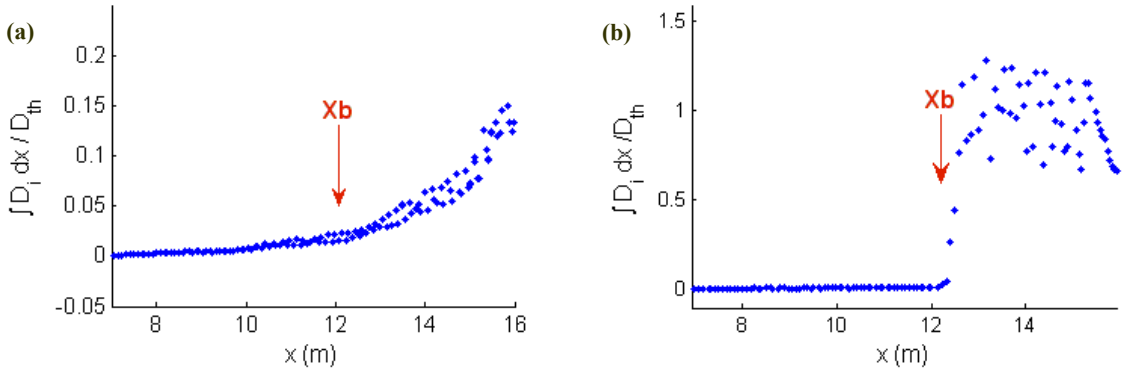

Figure 4. Normalized dissipation as a function of the position for the cnoidal wave propagation over a sloping beach (Ting and Kirby (1994) experiment). (a): without any treatment for wave breaking. (b): for x>Xb we switch to NSWE. (Xb: experimentally observed breaking point),

A mixed breaking criterion

The study of the energy dissipation needs to be combined with a criterion for the initiation of breaking. We use here a criterion based on the front slope, initially introduced by Schäffer et al. 1993. Two angles are then defined. Φi corresponds to the angle at which the breaking process starts, and Φf, the angle at which the breaking process stops. We choose Φi=30° and Φf=8°, which are the optimal angles determined by Cienfuegos et al. 2010 for their S-GN model.

Finally, the following method is applied in order to handle wave breaking at each time step. Potentially breaking wave fronts are first located thanks to the energy dissipation. For each of them, we compute the value of the front slope and the normalized dissipation. Finally, we decide if we switch locally from one set of equations to the other depending on the values of these two parameters:

If $\int_{front} D_i(x,t)dx/D_{th} > 0.5$ and Φ>Φf: the wave is broken and will keep breaking (as long as Φ> Φf) .

If $\int_{front} D_i(x,t)dx/D_{th} \leq 0.5$ and Φ<Φi: the wave is not breaking. The wave front is governed by S-GN equations. The switch to NSWE will eventually occur if Φ gets larger than Φi.

As several wave fronts can be detected at each time step, either breaking or not, the width of the zone (centred on the peak of dissipation) where the switch to NSWE is performed needs to be defined. It must be of the order of magnitude of the physical length of the roller, which is roughly proportional to the wave height. For the following test cases, we choose $l_{front} \approx 8H$. Further studies are necessary in order to determine an optimal value of l_{front}, in particular for test cases involving the propagation of irregular wave fronts.

The transition between the two systems is performed abruptly, without any smooth transition zone. In this way, wave propagation is governed by one given set of equations in each cell, and not by a non-physical mix of both sets. The transition generates some disturbances, but they remain of small amplitude and do not lead to instabilities. No numerical filtering is applied. It is worth noting that the generation of oscillations is also observed for Boussinesq models based on the surface roller method when the extra-terms responsible for wave breaking are activated.

This method has two important advantages. There is no parameterization for the energy dissipation due to wave breaking, since it is implicitly predicted by the shock theory. We do no need any complex algorithm to detect and follow the waves, contrary to most of the Boussinesq-type models with an ad-hoc

parameterization for wave breaking. The detection and characterization of the waves at each time step is performed through the study of the energy dissipation.

VALIDATIONS

Cox experiment

In our first test case we consider Cox's regular waves experiment (1995). Cnoidal waves of relative amplitude H/h_0=0.29 and period T=2.2s were generated in the horizontal part of a wave flume, of depth h_0=0.4m. They were then propagating and breaking on a 1:35 plane beach. For this test case, synchronized time-series of free surface elevation are available at six locations, corresponding to wave gages located outside (L1 and L2) and inside (L3 to L6) the surf zone (see Figure 5). The experimental breaking point is located slightly shoreward to L2.

Figure 6 compares the experimental and numerical time-series for this experiment. It is worth noting that the time-series are in phase, demonstrating that wave celerity is accurately predicted by the model. We have a very good overall agreement concerning the shape of the waves, both in the shoaling and surf zone. In particular, the model is able to reproduce the typical saw-tooth profile in the inner surf zone.

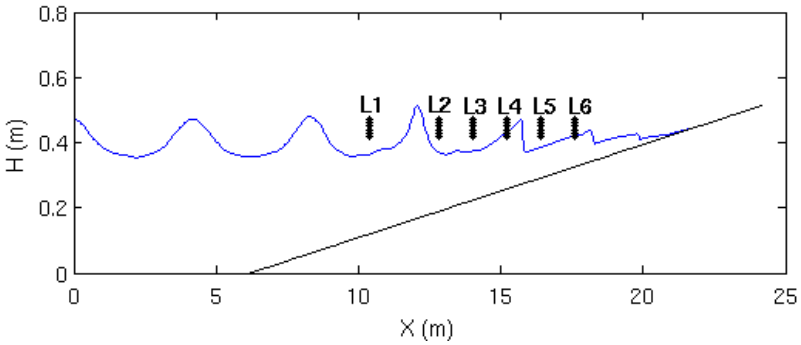

Figure 5. Definition sketch for Cox experiment (1995). Vertical lines (L1 to L6) correspond to the locations of the wave gauges. The free surface has been computed using the S-GN model.

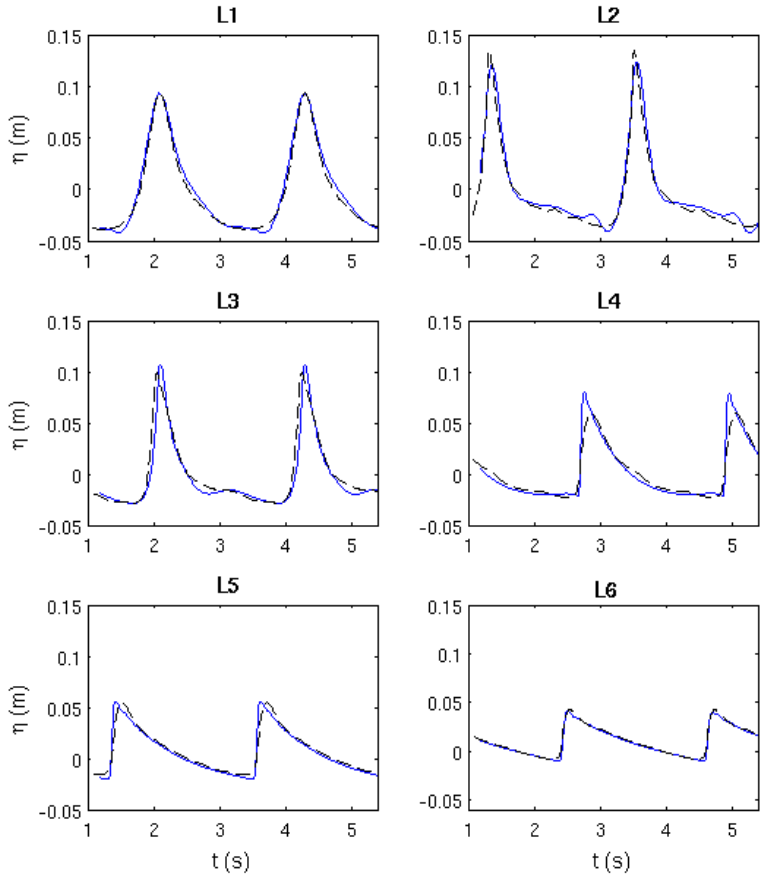

Figure 6. Comparisons of computed (blue lines) and experimental synchronized time-series of free-surface elevation at the wave gauges for Cox breaking experiment (1995).

Ting and Kirby experiment

In this section the numerical model is applied to reproduce the laboratory experiments performed by Ting and Kirby 1994. Cnoidal waves were generated in the horizontal part of a flume (h_0=0.4m) and were propagating over a 1:35 sloping beach. The wave period was T=2.0s and the incident wave height H=0.125m. For this experiment, non-synchronized time-series of surface elevations and mean characteristic levels (crest, trough and mean water levels) are available at 21 locations in the shoaling and surf zone. For the simulation, the grid size of the mesh is dx=0.05m and the time step is dt=0.02s.

Figure 7 shows the spatial variation of the crest and trough elevations, as well as the variation of the mean water level for experimental and numerical data. We can see that wave breaking is predicted a bit too early by our model. It explains the significant difference in both wave shape and amplitude observed in Figure 8 for the time-series at 12m, i.e. close to the breaking. The agreement between data and model predictions is good concerning the prediction of wave set-up, illustrating the fact that our model dissipates a realistic amount of energy. Figure 8 compares the time-series of free surface elevations at different locations. We can see that the wave asymmetry is accurately reproduced, even in the last stages of shoaling and in the Inner Surf Zone. The main discrepancies are found in the vicinity of the breaking point, but the overall agreement improves significantly while propagating shoreward. In particular, the wave height decay in the ISZ is well reproduced. A slight underestimation of wave shoaling can be observed in this test case.

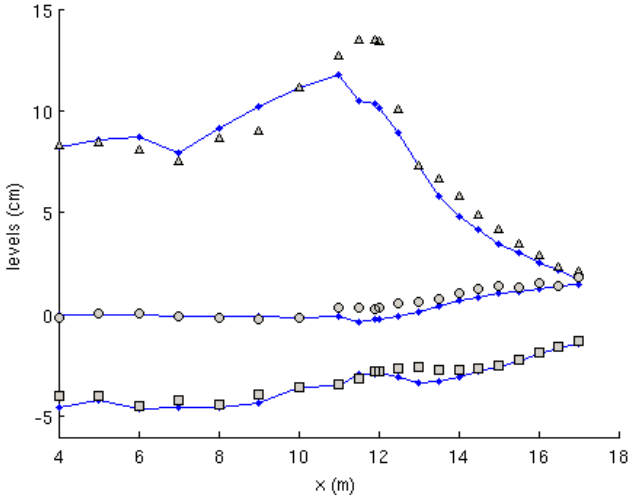

Figure 7. Comparisons of computed (blue lines) and experimental data (symbols) for Ting and Kirby experiment. (●) : Mean Water Level; (■): trough elevation relative to MWL; (▲): crest elevation relative to MWL.

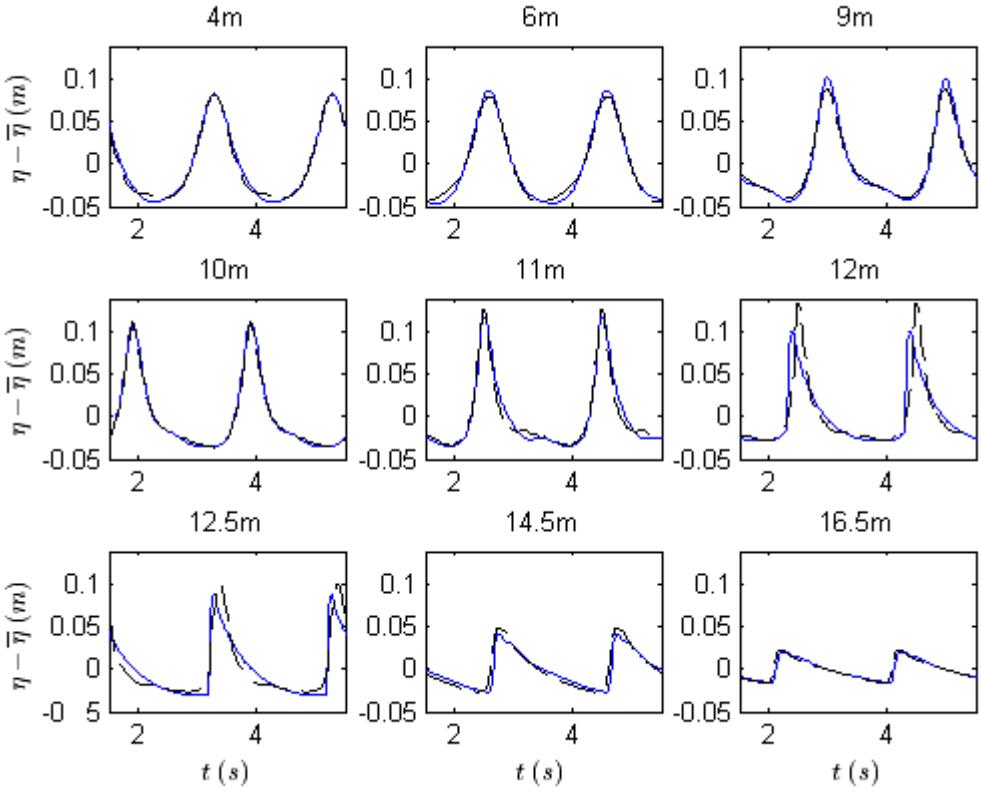

Figure 8. Comparisons of computed (blue lines) and measured (black dotted-lines) time-series of free surface elevations for Ting and Kirby experiment at different locations.

Synolakis experiment

In the last test case, we assess the ability of our model to describe wave breaking and shoreline motions. It is based on laboratory experiments carried out by Synolakis (1987) for an incident solitary wave of relative amplitude a_0/h_0=0.28, propagating and breaking over a planar beach with a slope 1:19.85. For this experiment, spatial snapshots at different times are available. The simulations are performed using the grid size dx=0.08m, and dt=0.02s. Bottom friction effects are expected to be important when the water becomes very shallow, i.e. during the run-up and run-down stages: a quadratic friction term is introduced for this simulation (friction coefficient f=0.002).

The comparisons between measured and computed waves are presented in Figure 9. We can see that the overall agreement is very good during shoaling, breaking, run-up and run-down. Moreover the model is able to describe the formation and breaking of a backwash bore, which is a particularly demanding test for most of Boussinesq-type models, since it involves broken bore propagating backward.

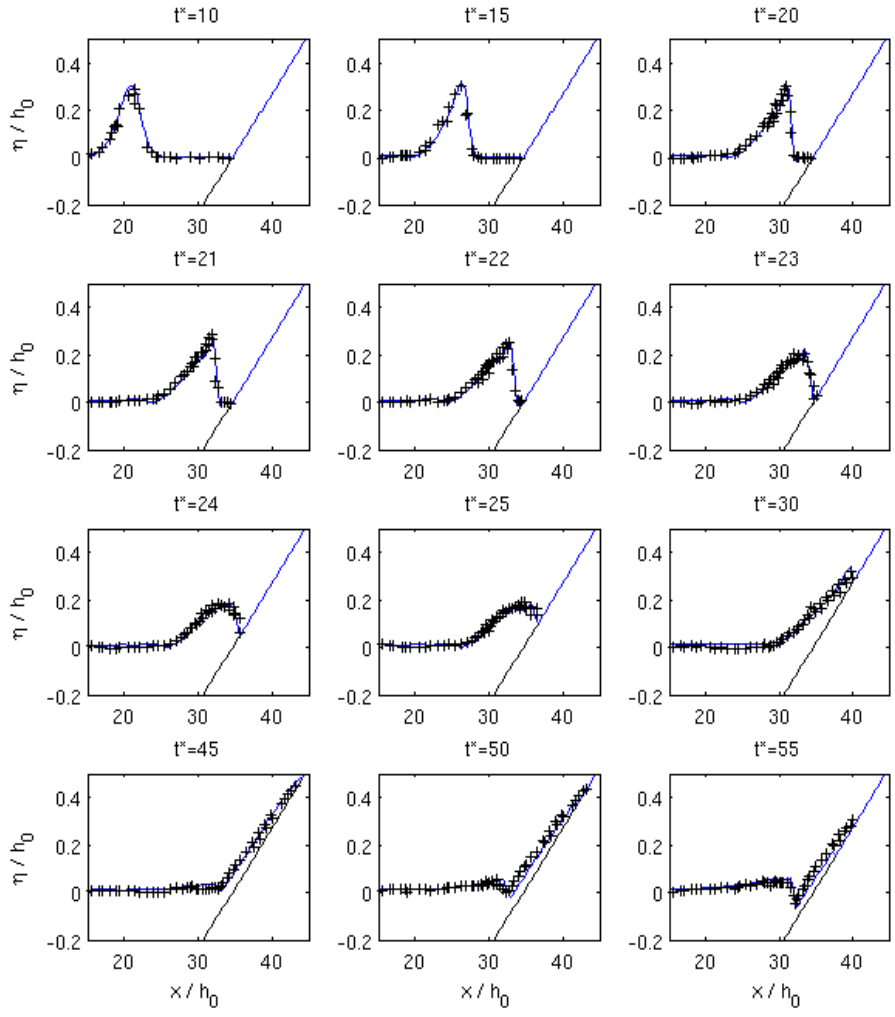

Figure 9. Comparisons of model predictions (blue lines) and experimental snapshots (+) for a breaking solitary wave with non-dimensional initial incident amplitude a_0/h_0=0.28, on a 1:20 plane beach (Synolakis (1987). $t^* = t(g/h_0)^{1/2}$.

CONCLUSIONS

In this paper, a fully non-linear weakly dispersive Green-Naghdi model is presented and successfully applied to the description of breaking waves and shoreline motions. This model has been developed as an extension of the well-validated NSW shock-capturing code SURF_WB (Marche et al 2007), using a time-splitting approach with hybrid schemes (Bonneton et al 2010a). The modelling strategy for wave breaking is based on the decomposition of S-GN equations between an hyperbolic part corresponding to the NSWE and a dispersive term. When the wave is ready to break, we switch locally to the NSWE by skipping the dispersive step, so as broken waves can be described as shocks. Energy dissipation due to wave breaking is then predicted by the shock theory, without needing any ad-hoc parameterization.

The detection and characterization of wave fronts at each time step are easily performed through the study of local energy dissipation. Combined with a commonly-used criterion based on the roller slope for the initiation and cessation of breaking, we obtain an efficient treatment for wave breaking and broken waves propagation without any complex algorithm to follow the waves.

Our method has been extensively validated for the breaking of regular waves. Additional work remains to be done concerning the validation for irregular wave fields. This model could then be a powerful tool to study submersion problems. In particular, preliminary tests suggest that it could efficiently be applied to overtopping problems.

Work is in progress concerning the 2HD extension of our model. This extension should be relatively straightforward since SURF_WB is already a well-validated up-to-date 2HD code, able to accurately describe broken waves propagation. The new 2HD S-GN code could be a very powerful tool to study the generation of wave-induced mean current vorticity in the surf zone (Castelle et al. 2010). Indeed, it has been showed that the dissipation gradients linked to differential breaking are a forcing mechanism for the generation of macrovorticity (Bonneton et al. 2010c).

ACKNOWLEDGMENTS

This work has been supported by the ANR MathOcean and by the project ECOS-CONYCIT. PhD thesis of M. Tissier is founded by MISEEVA (ANR).

REFERENCES

Audusse, E., F. Bouchut, M.-0. Bristeau, R. Klein and B. Perthame. 2004. A fast and stable well-balanced scheme with hydrostatic reconstruction for shallow water flows. *SIAM Journal on Scientific Computing*, 25(6), 2050-2065.

Berthon, C. and F. Marche, A positive preserving high order VFRoe scheme for shallow water equations: A class of relaxation schemes. 2008. *SIAM Journal of Scientific Computing*, 30(5), 2587-2612.

Bonneton, P. 2007. Modelling of periodic wave transformation in the inner surf zone, *Ocean Engineering*, 34, 1459-1471.

Bonneton, P., F. Chazel, D. Lannes, F. Marche and M. Tissier. 2010a. A splitting approach for the fully nonlinear and weakly dispersive Green-Naghdi model, *in correction to Journal of Computational Physics.*

Bonneton, P., E. Barthélemy, J.D. Carter, F. Chazel, R. Cienfuegos, D. Lannes, F. Marche, M. Tissier. 2010b. Fully nonlinear weakly dispersive modelling of wave propagation, breaking and run-up, *in correction to European Journal of Mechanics, B/Fluids.*

Bonneton P., N. Bruneau, F. Marche, B. Castelle. 2010c. Large-scale vorticity generation due to dissipating waves in the surf zone, *DCDS-S*, 13(4), 729-738.

Brocchini, M. and N. Dodd. 2008. Nonlinear Shallow Water Equation Modeling for Coastal Engineering, *J. Wtrwy., Port, Coast., and Oc. Engrg.*, 134(2), 104-120.

Bruno, D., F. De Serio and M. Mossa. 2009. The FUNWAVE model application and its validation using laboratory data, *Coastal Engineering*, 56(7), 773-787.

Castelle, B, H. Michallet, V. Marieu, F. Leckler, B. Dubardier, A. Lambert, C. Berni, P. Bonneton, E. Barthélemy and F. Bouchette, 2010. Laboratory experiment on rip current circulations over a moveable bed: drifter measurements, *in revision to Journal of Geophysical Research.*

Chazel, F., D. Lannes, F. Marche. 2010. Numerical simulation of strongly nonlinear and dispersive waves using a Green-Naghdi model*, Journal of Scientific Computing*, DOI: 10.1007/s10915-010-9395-9.

Cienfuegos, R., E. Barthélemy, and P. Bonneton. 2006. A fourth-order compact finite volume scheme for fully nonlinear and weakly dispersive Boussinesq-type equations. Part I: Model development and analysis. *Int. J. Numer. Meth. Fluids*, 56, 1217-1253.

Cienfuegos, R., E. Barthélemy and P. Bonneton. 2010. A wave-breaking model for Boussinesq-type equations including roller effects in the mass conservation equation. *J. Wtrwy., Port, Coast., and Oc. Engrg.,* 136(1), 10-26.

Cox, D. 1995. Experimental and numerical modelling of surf zone hydrodynamics. *PhD thesis, University of Delaware, Newark, Del.*

Kennedy, A.B., Q. Chen, J.T. Kirby and R.A. Dalrymple. 2000. Boussinesq modelling of wave transformation, breaking and runup. I:1D. *J. Wtrwy.,Port,Coast., and Oc. Engrg.*,119, 618-638.

Kobayashi, N., G. De Silva and K. Watson. 1989. Wave transformation and swash oscillation on gentle and steep slopes, *Journal of Geophysical Research,* 94, 951-966.

Lannes, D., and P. Bonneton. 2009. Derivation of asymptotic two-dimensional time-dependent equations for surface water wave propagation, *Physics of Fluids*, 21(1).

Madsen, P.A., 0.R. Sørensen and H.A. Schäffer. 1997. Surf zone dynamics simulated by a Boussinesq type model. Part I. Model description and cross-shore motion of regular waves, *Coastal Engineering*, 32, 255-287.

Marche, M., P. Bonneton, P. Fabrie and N. Seguin. 2007. Evaluation of well-balanced bore-capturing schemes for 2D wetting and drying processes, *Int. J. Num. Meth. Fluids*, 53(5), 867-894.

Schäffer, H.A., P. A. Madsen and R. Deigaard. 1993. A Boussinesq model for waves breaking in shallow water, *Coastal Engineering*, 20, 185-202.

Synolakis, C. E.. 1987. The run-up of solitary waves. *Journal of Fluid Mechanics*, 185, 523-555.

Ting, F. and J. Kirby. 1994. Observation of undertow and turbulence in a laboratory surf zone. *Coastal Engineering*, 24, 51-80.